Extracting Physics from the Stochastic Gravitational Wave Background

Brittany Christy

(Dated: September 26, 2014)

A gravitational-wave background is expected to arise from the superposition of many gravitational-wave signals, which are too weak to detect individually, but which combine to create a "stochastic" gravitational-wave glow. By measuring the stochastic background, we can probe a wide range of interesting science, from neutron stars to the inflationary epoch shortly after the Big Bang. This project is focused on studying the stochastic gravitational wave background originating from compact binary coalescence sources that we hope to detect with the Advanced LIGO-Virgo detector network. In particular, we are in the process of developing software to analize data from the Advanced LIGO-Virgo network, using Baysian analysis with a Markov Chain Monte Carlo algorithm to estimate the parameters associated with the stochastic gravitational wave background. We have applied this technique to simulated LIGO data in order to show that it is possible to infer the parameters associated with star formation rate density. Future work will focus on making the software sensitive enough to extract information from tiny signals buried deep in the noise of real LIGO data.

I. INTRODUCTION

Space and time can be thought of as a single fabric, which can be warped and stretched by massive objects. This warping of spacetime is what we call gravity. Binary systems consisting of extremely massive objects such as neutron stars or black holes orbiting around a common center of mass cause spacetime to ripple outward, similar to the way ripples form in a pool of water. These ripples are what we call gravitational waves. Gravitational waves are produced by accelerating masses, similar to the way electromagnetic waves are produced by accelerating charges. Gravitational wave detectors are basically giant two-armed interferometers, which use laser interference to measure the relative change in arm length, or strain, caused by passing gravitational waves. There are currently two gravitational wave detectors in the United States, known collectively as LIGO [1]. Initial LIGO was made more sensitive and updated to Advanced LIGO, which has increased the sensitivity by a factor of 10 [5].

The superposition of many localized, unresolved, and independent gravitational wave sources makes up the stochastic gravitational wave background (SGWB). The word "stochastic" means that though most of the sources are too weak to be detected individually, we can still analyze them statistically. One source of this background is compact binary coalescences or CBCs, which are binary systems of neutron stars and/or black holes[11]. CBCs coalesce because gravitational waves carry energy away from the system, in a three step process consisting of coalescence, merger, and ringdown. As two compact objects get closer together, the rate at which they orbit each other increases due to conservation of angular momentum, causing the frequency and amplitude of the emitted gravitational waves to increase as well. The eventual collision and merging of a CBC produces the strongest burst of gravitational waves, known as a "chirp". This gravitational wave frequency evolution is determined by a quantity known as the chirp mass [7], defined as

$$M_c = \frac{(M_1 M_2)^{\frac{3}{5}}}{(M_1 + M_2)^{\frac{1}{5}}}. \quad (1)$$

Nearby compact binary coalescences are expected to produce gravitational waves signals strong enough to be detected individually by second generation GW detectors. We can integrate all contributions from all compact binary coalescences to define a stochastic gravitational wave background from CBC sources that may be possible to detect with cross correlated pairs of detectors such as Advanced LIGO.

The theory for our CBC model predicts that the characteristics of the stochastic gravitational wave signals we expect to detect will largely depend on the universal binary neutron star formation rate and mass distribution.[10]. Once LIGO is sensitive enough to extract these signals from the noise, we can then work backwards to estimate these parameters by applying statistical inference methods to the data. This parameter estimation process will work the same way for all SGWB models, since each one is predicted to have a unique signal with characteristics dependent on specific parameters. These parameters are rooted in the physics of the sources, which means that estimating their values will help us gain a better understanding of the underlying physics governing the formation and characteristics of neutron stars, black holes, and other gravitational wave sources. This research will give us new information about the properties that govern our universe, including gravity itself.

II. THEORY

A. Understanding Coalescing Binary Black Hole Waveforms

The purpose of the following section is to illustrate the dependence of gravitational wave signal characteristics on the underlying physical parameters of their sources. Given an input of binary black hole system parameters such as mass ratio, radial distance, and observational distance, a script generated the following time and frequency waveforms to show how the behavior of the system changes with various configurations.

1. *Varying Mass Ratio*

When varying the mass ratio $\frac{m1}{m2}$, I smaller mass ratios result in longer coalescence times, as well as reduced gravitational wave strain overall. This makes sense, because the black holes in a two body system orbit around their common center of mass, known as the barycenter. If the two bodies are very unequal in size, the barycenter will be very close to the larger body, possibly even inside it. In this case the larger body does not accelerate as much as the smaller body, resulting in less total mass acceleration overall. This means that there is not enough mass accelerating to create strong gravitational waves, which results in a longer coalescence time, and decreased gravitational wave strain. Mass ratios closer to 1 maximize the amount of mass accelerating in the system, producing gravitational waves with large strain amplitude. These gravitational waves quickly carry energy away from the system, causing the two bodies to rapidly coalesce.

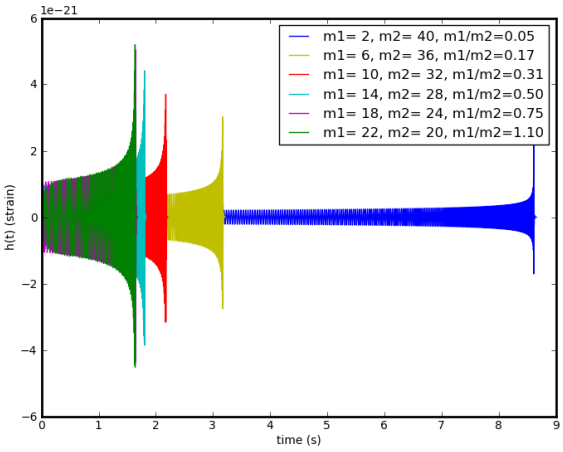

FIG. 1: Time domain waveform of binary black hole coalescence given different mass ratios.

The frequency domain waveform shows that CBCs with smaller mass ratios have lower frequency during coalescence, while systems with mass ratios closer to 1 have higher frequencies. It can also be seen that all systems spend more time at lower frequencies than higher frequencies, which makes sense because the inspiral and merger phase of CBCs only lasts minutes, a small fraction of the total lifespan of the CBC.

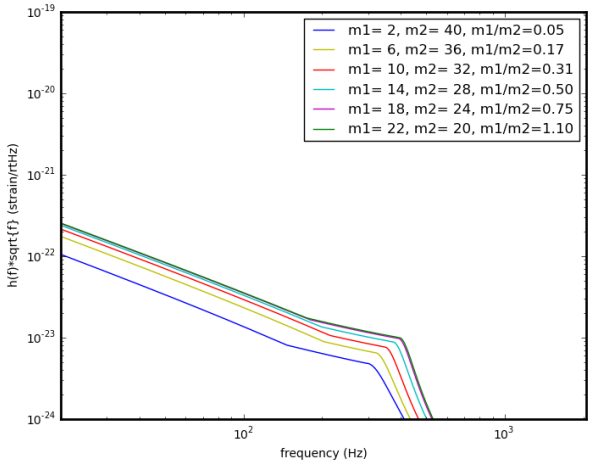

FIG. 2: Frequency domain waveform of binary black hole coalescence given different mass ratios.

2. *Varying Total Mass*

When varying the total amount of mass, systems with greater total mass coalesced more quickly, and had greater gravatational wave strain overall. Systems with greater total mass also coalesced at higher frequencies. This makes sense when considering that gravitational wave strain is directly proportional to the amount of total accelerating mass.

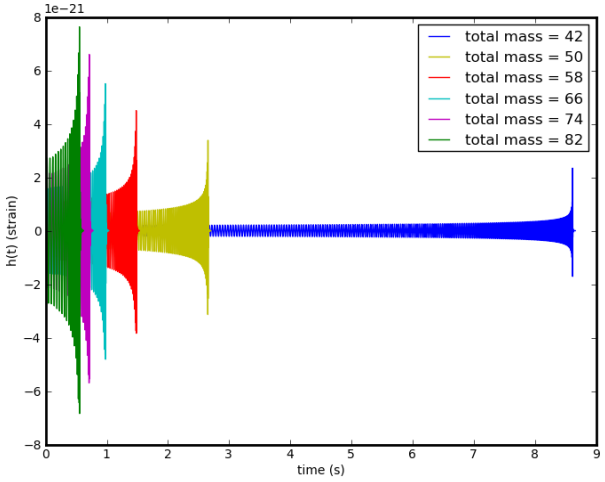

FIG. 3: Time domain waveform of binary black hole coalescence with varying total mass.

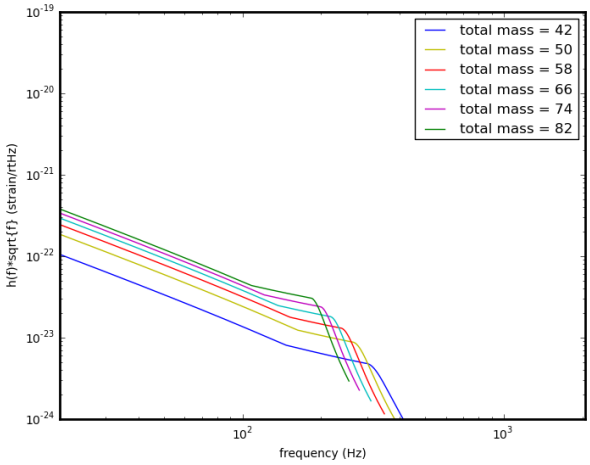

FIG. 4: Frequency domain waveform of binary black hole coalescence with varying total mass.

3. *Varying Observational Distance*

When varying observational distance from the system, gravitational wave strain decreased for far away CBC systems. This makes sense because we know that the amplitude of a gravitational wave falls off proportional to $\frac{1}{r}$, where r is the system's distance from the observer due to gravitational red shifting [12].

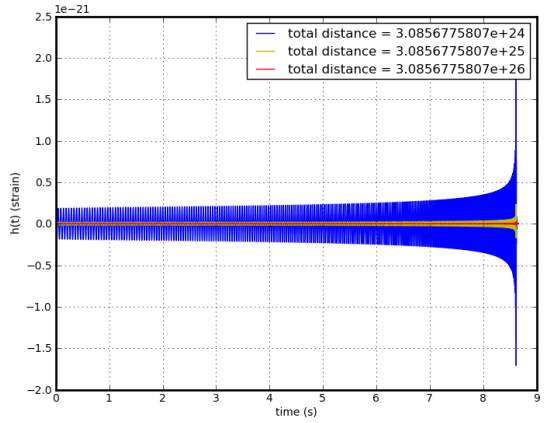

FIG. 5: Time domain waveform of binary black hole coalescence with varying observational distance.

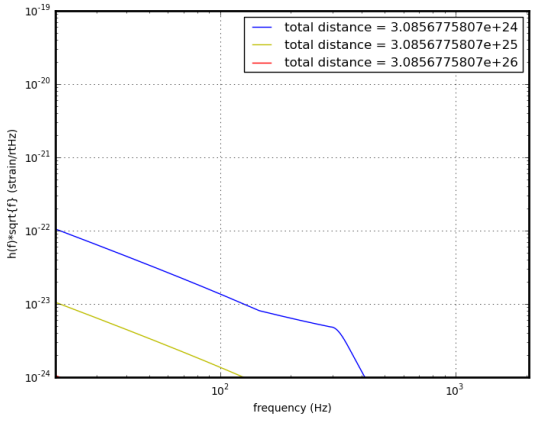

FIG. 6: Frequency domain waveform of binary black hole coalescence with varying observational distance.

B. Modeling the Stochastic Gravitational Wave Background

1. *Gravitational Wave Energy Density*

The stochastic gravitational wave background contains the distinct signatures of the physical processes that generated it. All SGWB source models, including CBCs, can be described by the normalized gravitational wave energy density,

$$\Omega_{GW}(f) = \frac{f}{\rho_c}\frac{dp_{GW}}{df}, \tag{2}$$

which defines the ratio of the model's gravitational wave energy density to the critical energy density needed for a flat universe, that is a universe that follows the rules of familiar Euclidean geometry[2]. In this equation, dp_{GW} is the energy density of gravitational waves in the frequency band $f \rightarrow f + df$, and ρ_c is the critical energy density needed for the universe to be flat.

2. *Compact Coalescing Binary Neutron Star Model*

Each SGWB model results in a different gravitational wave spectrum. For example, the gravitational wave spectrum for the CBC neutron star model is determined by the rate of binary neutron star system formation throughout the universe, as well as the mass distribution [10]. For this model, including only the inspiral part of the signal, we can write the gravitational wave spectrum Ω_{GW} as a double integral over redshift z and chirp mass M_c', as depicted in equation 3 below:

$$\Omega_{GW}(f;M_c,\lambda) = \frac{8\lambda(\pi G)^{5/3}f^{2/3}}{9H_0^3c^2}\int dM_c^{'}p(M_c^{'})M_c^{'5/3}\int_0^{Z_{sup(M_c^{'})}}\frac{R_V(z)dz}{(1+z)^{1/3}E(\Omega_M,\Omega_\Lambda,z)}$$
$$\approx \frac{8\lambda(\pi G M_c)^{5/3}}{9H_0^3c^2}f^{2/3}\int_0^{Z_{sup(M_c)}}\frac{R_V(z)dz}{(1+z)^{1/3}E(\Omega_M,\Omega_\Lambda,z)}. \quad (3)$$

This equation integrates the contributions of all CBCs distributed throughout the Universe. The simplified Ω_{GW} in the second line of equation 3 is obtained by approximating the first integral in the original Ω_{GW} equation with the average chirp mass M_c, assuming that the shape of the chirp distribution has very little effect on the gravitational wave spectrum at frequencies below LIGO sensitivity [10]. 7 illustrates a few examples of what this spectrum looks like for different average chirp mass parameters.

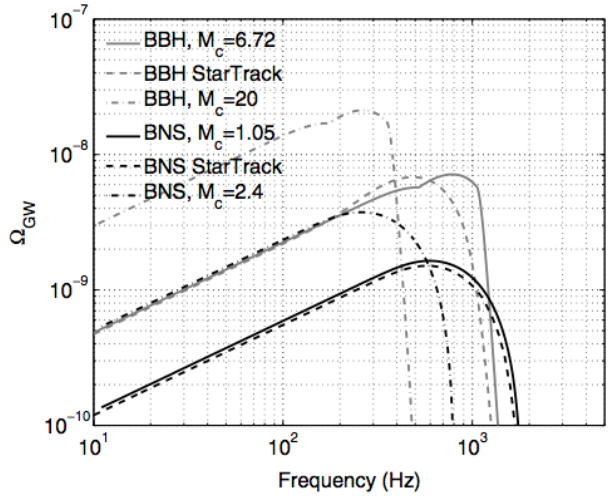

FIG. 7: [10] Gravitational wave spectrum Ω_{GW} example.

The mass fraction parameter λ is proportional to the local CBC formation rate per unit comoving volume, while $E(\Omega_M,\Omega_\Lambda,z) = \sqrt{\Omega_m(1+z^3)+\Omega_\Lambda}$ represents the dependence of the comoving volume on the redshift z caused by the accelerating expansion of the universe [10]. The term "comoving volume" refers to a constant volume obtained by factoring out universal expansion so that we can work with volumes that do not change over time due to the expansion of space. We do this so that celestial objects such as CBCs remain at fixed spacial coordinates in our calculations [9]. The expansion is taken care of by a scale factor, which is used to calculate comoving distances and volumes, as described in [6].

For our purposes, we also assume the Lambda Cold Dark Matter cosmology model, which says that our universe contains a Λ parameter describing the dark energy that causes accelerating expansion, as well as the cold dark matter detectable by its gravitational effects on regular matter. In addition, we use the flat-Λ cosmology values of 0.3 for the mass density parameter Ω_m, and 0.7 for the cosmological constant density parameter Ω_Λ [4]. Finally, $R_V(z)$ is the cumulative star formation rate denisty as a function of redshift z.

The upper limit of the integral in equation 3 depends on the $\Omega_{GW}(f)$ frequency range f_{min} to f_{max}, where f_{max} is the frequency of the last stable orbit before the merger[8],

$$f_{lso} = \frac{1}{6^{\frac{3}{2}}\pi M_c \eta^{-\frac{3}{5}}}, \quad (4)$$

and $\eta \approx 0.25$ is the reduced mass function assuming equal masses,

$$\eta = \frac{M_1M_2}{(M_1+M_2)^2}. \quad (5)$$

For this simplified Ω_{GW} equation, the prefactor outside the integral depends on the average chirp mass parameter M_c, which determines the signal strength or amplitude of the gravitational wave energy density spectrum Ω_{GW}. The integrand is dependent on the star formation density R_V, which determines the distribution of sources throughout the universe. For my project, we implemented the star formation rate R_V as a fit to the star formation rate density in Eq.7 of [4]. In addition to being a function of redshift, R_V is also dependent on the the parameters r_0, W, Q, and R, where r_0 is the local star formation rate in units of $Mpc^{-3}yr^{-1}$, and W, Q, and R are phenomenological parameters which describe the shape of the star formation rate denisty over redshift z [4],

$$R_V(z) \propto \frac{r_0(1+W)e^{Qz}}{e^{Rz}+W}. \quad (6)$$

C. Research Goal

The project goal was to estimate the parameters M_c, r_0, W, Q, and R of the gravitational wave spectrum for coalescing binary neutron stars. We are interested in doing this, because we want to better understand the star formation rate density which depends on the parameters r_0, W, Q, and R, and the neutron star mass distribution, which depends on the M_c parameter. Although observational astronomy has given us a good idea of the star

formation rate density (see Fig.8), our limited observational data and physical understanding of the universal CBC population makes it difficult to be certain of the true values.

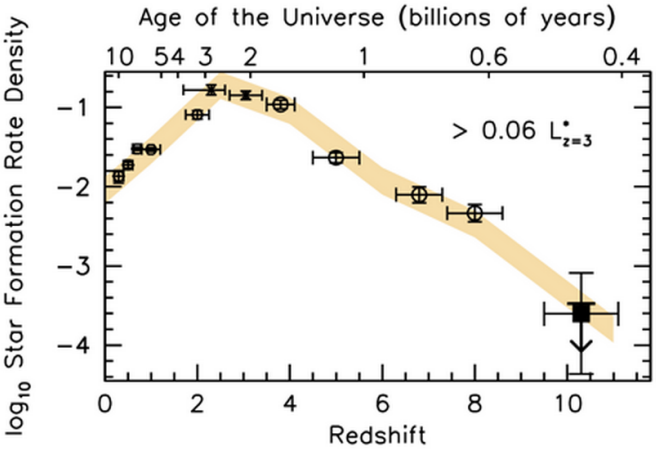

FIG. 8: Star formation rate density, [3]

D. Using Bayesian Inference to Estimate CBC Parameters

Bayesian parameter estimation methods use a combination of prior knowledge and experimental data to make the best possible inference. It is based on Bayes' law,

$$\overbrace{\Pr(\hat{\theta}|D)}^{\text{Posterior}} = \frac{\overbrace{\Pr(D|\hat{\theta})}^{\text{Likelihood}}\overbrace{\Pr(\hat{\theta})}^{\text{Prior}}}{\underbrace{\Pr(D)}_{\text{Evidence}}} \tag{7}$$

where θ represents the parameter to be estimated, such as average chirp mass M_c, and **D** represents the observational SGWB data gathered from LIGO. We can estimate the model parameter θ,by calculating the Bayesian posterior distribution $\Pr(\theta|\mathbf{D})$.

As described before, we are interested in estimating the parameters Mc, r0, W, Q, and R of the gravitational wave spectrum Ω_{GW} for coalescing binary neutron stars.

The first step of this process is to calculate the likelihood $\Pr(\hat{\Omega}|r_0)$, which represents the probability of the observational data from the LIGO detectors, given the value of the local star formation rate parameter r_0. The likelihood distribution is expected to be Gaussian because we calculate $\hat{\Omega}$, the cross correlation estimator for the measured output of the two LIGO gravitational wave detectors, by averaging over many short time segments. For our purposes the likelihood function can be defined as follows:

$$L(\vec{\theta}) \propto \exp\left[-\frac{1}{2}\sum_i \frac{[\hat{\Omega}_i - \Omega_{true}(f_i;\vec{\theta})]^2}{\sigma_i^2}\right], \tag{8}$$

where $\vec{\theta}$ denotes the model parameters we wish to estimate (r_0 in our simplified example), σ^2 is the varience of $\hat{\Omega}_i$, and Ω_{true} is the theoretically expected gravitational wave energy density given f and the true "expected" value for $\vec{\theta}$. Ω_{true} was derived using predicted values of the parameters r_0, W, Q, and R taken from [4]. Because most SGWB models vary very slowly with frequency, $\hat{\Omega}$ is approximated by computing each $\hat{\Omega}_i$ over a series of small $0.25Hz$ frequency intervals f_i.

For this research, I wanted clear results showing that my parameter estimation methods were working. Unfortunately, real LIGO data was too noisy for my first generation code to work with. Although future progress will require code sensitive enough to handle real data, for now it is sufficient to simulate $\hat{\Omega}$ and σ_i[1] by using expected values of the parameters r_0, W, Q, and R taken from [4], which I will refer to as the "true" values. When using a cross correlation estimator derived from real LIGO data, the true values of the parameters determined by the physics of the sources will be similarly embedded in the data, since it will be composed of signals from the real stochastic gravitational wave background.

In order to get the posterior distribution result, we multiply the likelihood by the prior, which is the previously known probability of r_0, and divide by the evidence $\Pr(\hat{\Omega})$ to normalize the result. In this case we begin by taking the prior to be flat within the range of r_0 and zero elsewhere. We don't include the evidence for now, because it does not depend on the parameter r_0 that we are estimating. The resulting Bayesian posterior distribution can be used to derive confidence intervals for the θ parameters we are estimating. [10]. A confidence interval gives an estimated range of values which is likely to include the unknown parameters $\vec{\theta}$, with this estimated range being calculated from a set of sample data.

E. Sampling the Likelihood Distribution Using Markov Chain Monte Carlo Methods

Because parameter estimation requires us to sample the values of $\vec{\theta}$ with the highest likelihoods, sampling the likelihood distribution turned out to be more difficult than anticipated. The problem stems from the fact that there is no obvious way to sample the likelihood without enumerating most or all of the possible states of our parameters, even in the case where $\vec{\theta}$ contains only one parameter r_0 [13]. Since good samples will by definition tend to come from places in the $\vec{\theta}$ space where the likelihood is high, how is it possible to identify $\vec{\theta}$ values where the likelihood is large without evaluating the likelihood everywhere by brute force? Sampling becomes costly and inefficient, because the calculation time to sample a distribution increases exponentially with the dimensionality

[1] See "Simulating Detector Data" (section IV C)

of $\vec{\theta}$. Since the goal is to estimate multiple parameters at once, it is necessary to use a non-brute force method. A common solution for a Baysian parameter estimation dilemma such as this is to use a Markov Chain Monte Carlo method to generate parameter samples. A Markov chain is a sequence of random variables that randomly moves from state to state over discrete units of time, while the term "Monte Carlo" refers to a computer generated algorithm that generates the Markov Chain. The key idea is to generate a Markov chain for each parameter that converges to the desired probability distribution, in this case the Ω_{GW} likelihood distribution in equation 8.

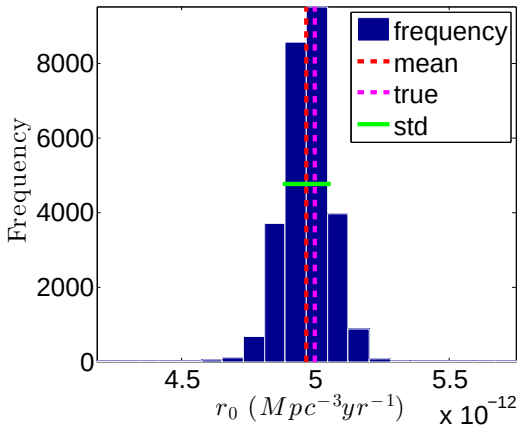

FIG. 9: MCMC Parameter estimation of r_0 parameter.

III. RESULTS

All parameter estimation results were obtained with an MCMC method called the Metropolis-Hastings algorithm[2]. Every parameter was assigned 100 identical Markov chain program "walkers" to sample the parameter space, with each walker given a unique random number seed to ensure that they would generate independent samples. After the walkers ran for 600 iterations, their samples were combined into one dataset of 600,000 values and plotted as a histogram.

My first test estimated only the r_0 parameter while keeping the other phenominological parameters W, Q, and R constant at their expected values. The following histogram shows the frequency of the r_0 samples generated by my MCMC algorithm for the Ω_{GW} likelihood distribution in equation 8. , for r_0 values in the range $[4 \times 10^{-12} - 6 \times 10^{-12}] Mpc^3 yr^{-1}$.

The histogram for the r_0 samples in figure 9 resembles a Gaussian, with a mean value that is very close to the true value of 5×10^-12 that was injected into the simulated detector data. This result seemed to indicate that the Metropolis-Hastings algorithm is working.

Next, I sampled all of the four star formation rate parameters r_0, W, Q, and R, with each walker sampling all four values at once. Unlike the previous outcome from sampling r_0 alone, the resulting histograms in figure 10 did not converge to clear Gaussian distributions centered on the true values. This could be because the different parameter samples are calculated all at once, making it harder for each individual parameter's chain to converge to the likelihood distribution. This issue might be resolved with the use of another MCMC algorithm. However, the most important thing to consider is that when reviewing each parameter's histogram result, it is clear that the mean value is still reasonably close to the true value of the parameter, which shows again that each parameter estimation result actually does correctly follow the likelihood distribution.

[2] See Markov Chain Monte Carlo Method()

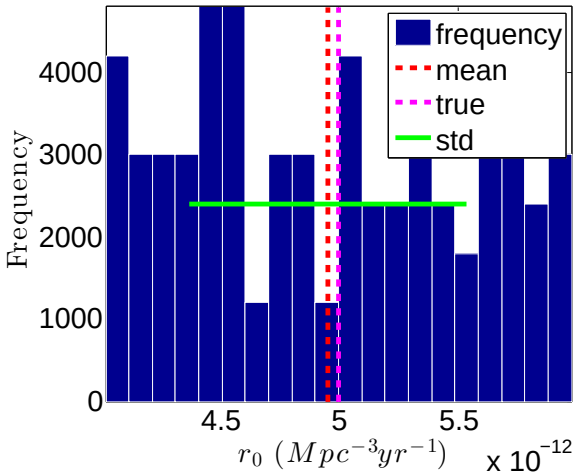

(a) MCMC multiple-parameter estimation of r0

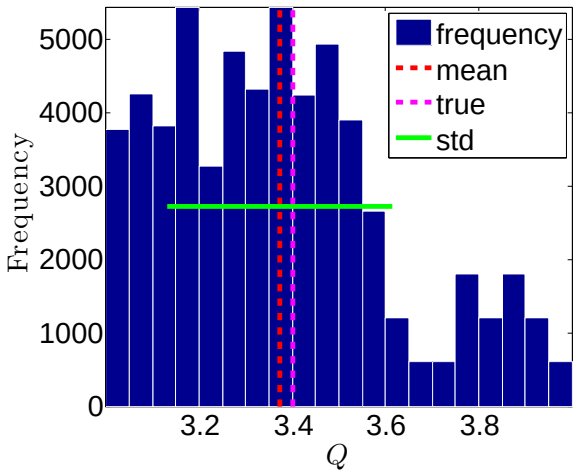

(b) MCMC multiple-parameter estimation of Q

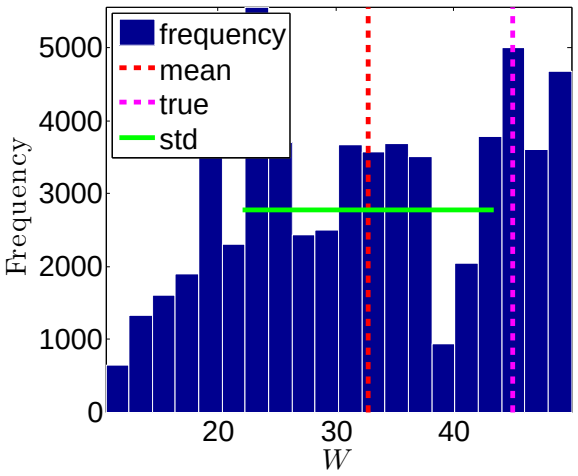

(c) MCMC multiple-parameter estimation of W

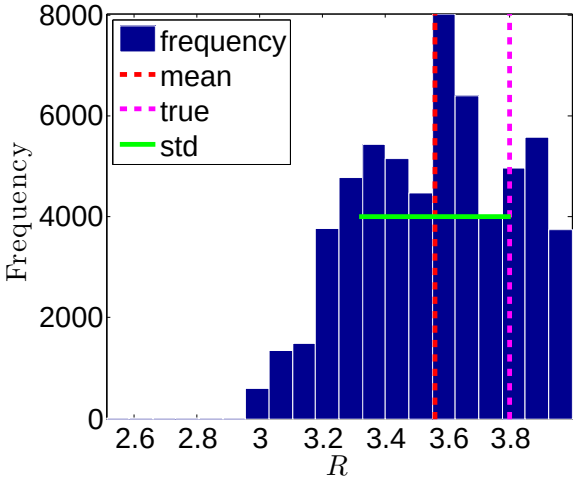

(d) MCMC multiple-parameter estimation of R

FIG. 10: Parameter estimation histograms for samples generated by using a Metropolis-Hastings algorithm to sample all four star formation rate density parameter spaces at once. The x-axis defines the range of the parameter in question, while the y-axis shows the frequency at which each parameter value was sampled by the MCMC algorithm. The four parameters r_0, Q, W,and R are used by the star formation rate density function $R_V(z)$ in the integrand of the CBC model's gravitational wave energy density spectrum Ω_{GW} in equation **??**. Star formation rate energy density influences the shape of Ω_{GW} by defining the density of CBC sources throughout the universe for a range of redshift values. The true parameter values injected into the simulated detector data $\hat{\Omega}$ are $(r_0, Q, R, W) = (5 \times 10^{-12}, 3.4, 3.8, 4.5)$, taken from the values used for star formation rate SF1 in [4].

Figure 11 is the result of using the calculated mean parameter estimation values in figure 10 to plot the star formation rate density $R_V(z)$. When comparing this curve to the $R_V(z)$ curve generated by using the true injected values $(r_0, Q, R, W) = (5 \times 10^{-12}, 3.4, 3.8, 4.5)$ in [4], it is clear that the curves are very similar. This shows that although the results are not perfect, the Metropolis-Hastings MCMC algorithm is functioning correctly.

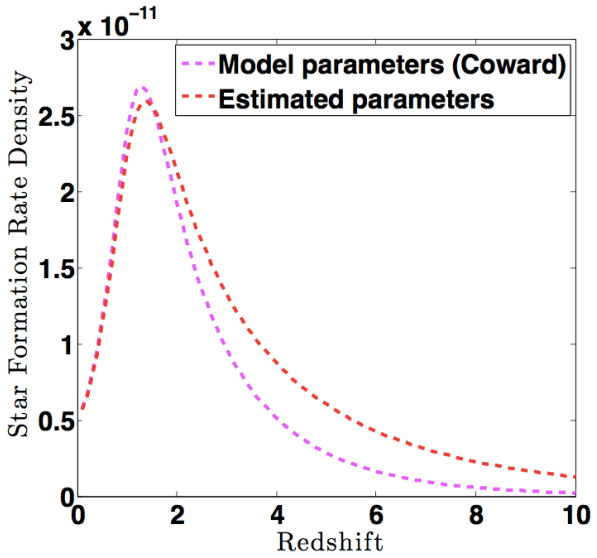

FIG. 11: Plots of star formation rate density for true parameter values vs. MCMC estimated parameter values.

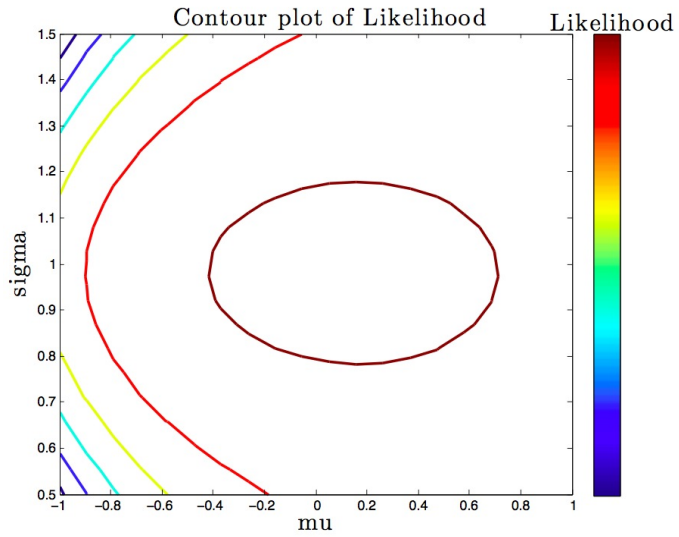

FIG. 12: Likelihood contour plot for gaussian distribution

IV. METHODS

A. Likelihood Calculations

The following is an example of how Gaussian likelihoods can be caluclated for two parameters σ and $\hat{\mu}$, assuming a Gaussian normal distribution, and using equation 9. The CBC likelihood in equation **??** was calculated using the same methods, with respective variables replaced.

$$L(x_i|\hat{\mu},\sigma) = \frac{1}{\sigma\sqrt{2\pi}} e^{-\frac{1}{2}\left(\frac{x_i-\hat{\mu}}{\sigma}\right)^2} \tag{9}$$

To do this, I first created a vector $\vec{x}$ from $10,000$ values chosen randomly from a normal distribution, with $\mu = 0$ and $\sigma = 1$. I then created vectors $\vec{\mu}$ and $\vec{\sigma}$ of length N with ranges from $(-1, 1)$ and from $(0.5, 1.5)$ repectively. The final likelihood value $L(\vec{x}|\hat{\mu}_j, \sigma_k)$ for each (μ_j, σ_k) pair, $1 \leq j, k \leq N$, is the product

$$L(x_i|\hat{\mu}_j,\sigma_k) = \left(\frac{1}{\sigma\sqrt{2\pi}}\right)^N e^{-\frac{1}{2}\sum_i\left(\frac{x_i-\hat{\mu_j}}{\sigma_k}\right)^2}. \tag{10}$$

In order to make the likelihoods easier to plot, the log likelihood was used:

$$\log L(x_i|\hat{\mu}_j,\sigma_k) = N\log\frac{1}{\sigma\sqrt{2\pi}} - \frac{1}{2}\sum_i\left(\frac{x_i-\hat{\mu_j}}{\sigma_k}\right)^2 \tag{11}$$

After calculating the log likelihoods for each (μ_j, σ_k) pair, I end up with a matrix of likelihood values, which I plotted on a 2D contour plot as shown in Fig 12:

In Fig. 12, The x and y axis' are the range of μ_j and σ_k, and the z axis is the likelihood value for this (μ_j, σ_k) pair. The highest likelihood occurs when $\sigma = 1$ and $\mu = 0$, which makes sense because the vector $\vec{x}$ was generated with these mean and standard deviation values. This represents the brute force likelihood calculation for parameter estimation of the two parameters μ and σ.

B. Sampling Likelihood Function Using Markov Chain Monte Carlo Method

I chose to sample the previous likelihood distribution of the same two variables μ and σ using an MCMC method called the Metropolis-Hastings algorithm to generate samples from a given probability distribution $P(x)$. This method was extended and altered to generate samples from the CBC likelihood probability distribution in equation 8.

The Metropolis-Hastings algorithm is used to generate a sequence of random samples $\vec{x}$ from a desired distribution $P(x)$ for which direct sampling is too difficult or time consuming. The algorithm does this by starting with an initial x value $x(t)$, and assuming that we can evaluate $P^*(x)$ for any x. A new state $x^{'}$ is generated from a proposal density $Q(x)$. To decide whether to accept the new state $x^{'}$, we calculate the quantity

$$a = \frac{P^*(x^{'})}{P^*(x(t))}\frac{Q(x(t);x^{'})}{Q(x^{'};x(t))}, \tag{12}$$

where the Q ratio cancels out if the proposal distribution Q is symmetric. If $a \geq 1$, then we accept $x^{'}$ as the new state. Otherwise, the new state $x^{'}$ is accepted with probability a.

Finally, if $x^{'}$ is accepted, we set $x^{'}(t+1) = x^{'}$. If $x^{'}$ is rejected, we set $x(t+1) = x(t)$.

The Matlab code implementing the Metropolis-Hastings algorithm for the previously plotted gaussian likelihood distribution over μ and θ is included in the appendix, which shows the algorithm edited to sample the Gaussian likelihood distribution over two parameters instead of one, and using the log-likelihood instead of the original likelihood equation for plotting purposes.

The results below in figure 13 are similar to the results from doing the brute force likelihood sampling method in figure 12:

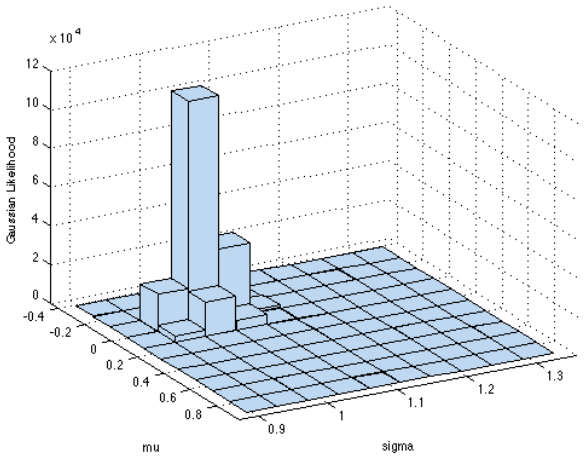

FIG. 13: Likelihood histogram of μ and σ for a Gaussian likelihood distribution.

C. Simulating Detector Data

In order to simulate the cross-correlated detector data $\hat{\Omega}$, we first need to correctly calculate Ω_{GW}, the "true" gravitational wave energy density based on our theoretically expected parameter values of $(r_0, Q, R, W) = (5 \times 10^{-12}, 3.4, 3.8, 4.5)$. These values are taken from the values used for star formation rate SF1 in [4]. Next, we calculate $\sigma_\Omega(f)$, the standard deviation of $\hat{\Omega}$:

$$\sigma_\Omega(f) = \frac{P(f)}{\frac{1}{5}\gamma(f)} f^3 \frac{2\pi^2}{3H_0^2} \sqrt{\frac{1}{T\delta f}}, \tag{13}$$

,

where $P(f)$ is the power spectral density $(\frac{strain^2}{Hz})$ plotted in figure 15, $\gamma(f)$ is the overlap reduction function for the two LIGO detectors plotted in figure 14, H_0 is the Hubble constant, T is the length of observation time, and δf is the frequency step size. Finally, the simulated $\hat{\Omega}$ can then be calculated by generating a vector of normally distributed random numbers with mean $\mu = \Omega_{GW}(f)$, and standard deviation $\sigma = \sigma_\Omega(f)$.

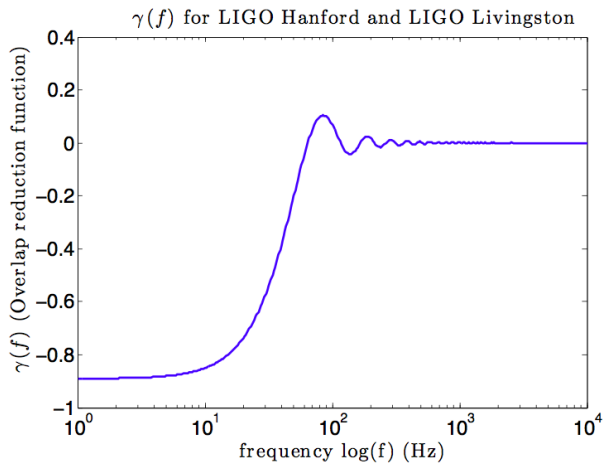

FIG. 14: Overlap reduction function $\gamma(f)$ for LIGO Hanford and LIGO Livingston detectors

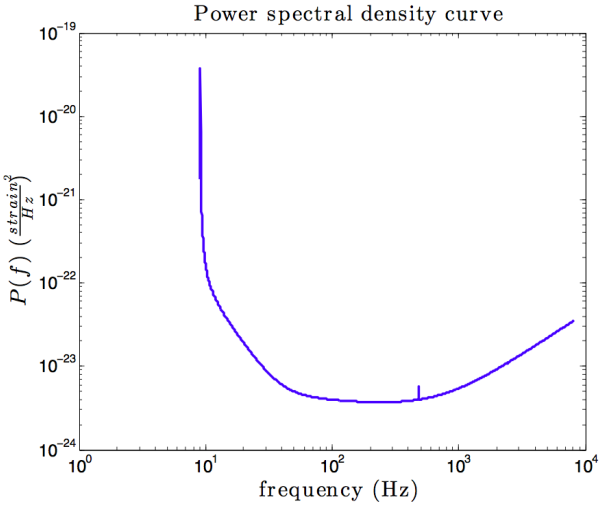

FIG. 15: Power spectral density curve for Advanced LIGO.

V. Conclusion and Future Work

Although the above results are promising, they are not based on realistic input. Unfortunately, none of the results from my initial runs of the Metropolis-Hastings algorithm converged to the likelihood distribution at all. In order to get the samples to converge to the results described previously, I ended up having to simulate the cross-correlation estimator $\hat{\Omega}$ again, this time without any noise. Originally, $\hat{\Omega}$ was calculated as a random vector with mean values equal to my theoretical $\vec{\Omega_{true}}$ and varience values equal to my simulated $\vec{\sigma}$, with $\vec{\sigma}$ based on

the LIGO noise curve[3]. Getting rid of the noise means that $\hat{\Omega}$ is equal to $\vec{\Omega_{true}}$, which is not ideal for real parameter estimation using LIGO data.

Even after I took the noise out of $\hat{\Omega}$, it was still necessary to divide the simulated varience σ used in 8 by 100 to get clear results. In conclusion, the previous results in figures 9 and 10 were based on a cross-correlation estimator based on a noiseless $\hat{\Omega}$ as well as a reduced σ. These problems mean that the Metropolis-Hastings algorithm needs to be made more sensitive so that it can can support simulated noise input. It might also be beneficial to consider using another MCMC algorithm altogether, depending on whether the current algorithm can be altered to handle realistic data.

VI. Appendix

A. Markov Chain Monte Carlo Implementation Example

```
%% Start sampling
while t < T % Iterate until we have T samples
    t = t + 1;

    % propose new values for mu & sigma from uniform random proposal distribution Q
    new_mu = unifrnd( mu_min(1) , mu_max(1) ); % mu'
    new_sigma = unifrnd( sigma_min(2) , sigma_max(2) ); % sigma'
    log_a = gaussianLikelihood( x, new_mu, new_sigma)-gaussianLikelihood(x,mu,sigma);
    if log_a >= 0
        % accept state
        mu = new_mu;
        sigma = new_sigma;
    else
        % accept state with probability a
        u = rand; % get a random number from 0-1
        if log(u)<log_a
            mu = new_mu;
            sigma = new_sigma;
        end
    end

    state(1,t) = mu;
    state(2,t) = sigma;

end
```

Acknowledgments

I'd like to acknowledge my mentors Tjonnie Li and Eric Thrane for helping me throughout the summer. I'd also like to acknowledge Alan Weinstein for his support and encouragement, as well as LIGO, Caltech, and the NSF for funding my project and giving me the opportunity to be a part of this research. Lastly I'd like to acknowledge my fellow interns for lending their support and help when I got stuck. Thank you!

[1] Advanced ligo – the next step in gravitational wave astronomy.

[2] Bruce Allen and Joseph D Romano. Detecting a stochastic background of gravitational radiation: Signal processing strategies and sensitivities. *Physical Review D*, 59(10):102001, 1999.

[3] RJ Bouwens, GD Illingworth, I Labbe, PA Oesch, M Trenti, CM Carollo, PG van Dokkum, M Franx, M Stiavelli, V González, et al. A candidate redshift z [thinsp][ap][thinsp] 10 galaxy and rapid changes in that population at an age of 500 [thinsp] myr. *Nature*, 469(7331):504–507, 2011.

[4] DM Coward and RR Burman. A cosmological 'probability event horizon'and its observational implications. *Monthly Notices of the Royal Astronomical Society*, 361(1):362–368, 2005.

[5] Gregory M Harry, LIGO Scientific Collaboration, et al. Advanced ligo: the next generation of gravitational wave detectors. *Classical and Quantum Gravity*, 27(8):084006, 2010.

[3] See calculating the noise curve (section IV C)

[6] David W Hogg. Distance measures in cosmology. *arXiv preprint astro-ph/9905116*, 1999.
[7] T.G.F. Li. Extracting physics from gravitational waves.
[8] TGF Li, W Del Pozzo, S Vitale, C Van Den Broeck, M Agathos, J Veitch, K Grover, T Sidery, R Sturani, and A Vecchio. Towards a generic test of the strong field dynamics of general relativity using compact binary coalescence. *Physical Review D*, 85(8):082003, 2012.
[9] Andrew Liddle. *An introduction to modern cosmology*. John Wiley & Sons, 2013.
[10] Vuk Mandic, Eric Thrane, Stefanos Giampanis, and Tania Regimbau. Parameter estimation in searches for the stochastic gravitational-wave background. *Physical review letters*, 109(17):171102, 2012.
[11] BS Sathyaprakash and Bernard F Schutz. Physics, astrophysics and cosmology with gravitational waves. *Living Reviews in Relativity*, 12(2), 2009.
[12] Alan Weinstein. Gravitational waves and ligo. Powerpoint Lecture, 6 2002.
[13] Yuhong Yang. Information theory, inference, and learning algorithms. *Journal of the American Statistical Association*, 100(472):1461–1462, 2005.